Available online at www.sciencedirect.com
ScienceDirect
Proceedings of the Combustion Institute 33 (2011) 3211–3218
Proceedings of the Combustion Institute
www.elsevier.com/locate/proci

Effects of non-equilibrium plasma discharge on counterflow diffusion flame extinction

Wenting Sun [a], Mruthunjaya Uddi [a], Timothy Ombrello [b], Sang Hee Won [a], Campbell Carter [b], Yiguang Ju [a,*]

[a] Department of Mechanical and Aerospace Engineering, Princeton University, Princeton, NJ 08544, USA
[b] U.S. Air Force Research Laboratory, Propulsion Directorate, Wright-Patterson AFB, OH 45433, USA

Abstract

A non-equilibrium plasma assisted combustion system was developed by integrating a counterflow burner with a nano-second pulser to study the effects of atomic oxygen production on the extinction limits of methane diffusion flames at low pressure conditions. The production of atomic oxygen from the repetitive nano-second plasma discharge was measured by using two-photon absorption laser-induced fluorescence (TALIF). The results showed that both the atomic oxygen concentration production and the oxidizer stream temperature increased with the increase of the pulse repetition frequency for a constant plasma voltage. The experimental results revealed that the plasma activated oxidizer significantly magnified the reactivity of diffusion flames and resulted in an increase of extinction strain rates through the coupling between thermal and kinetic effects. Numerical computations showed that atomic oxygen quenching strongly depends on the oxidizer stream temperature. The kinetic effect of atomic oxygen production by a non-equilibrium plasma discharge on the enhancement of flame extinction limits was demonstrated, for the first time, at high repetition frequencies with elevated oxidizer temperatures. The reaction paths for radical production and consumption were analyzed. It was concluded that in order to achieve significant kinetic enhancement from atomic oxygen production on flame stabilization, the plasma discharge temperature needs to be above the critical crossover temperature which defines the transition point from radical termination to chain-branching.

Keywords: Plasma assisted combustion; Atomic oxygen; TALIF; Counterflow extinction

1. Introduction

Over the last few years, plasma assisted combustion has drawn considerable attention for its potential to enhance combustion performance in gas turbine and scramjet engines. Significant progress has been made in developing new techniques of plasma discharges and in understanding the mechanisms of the plasma-flame interaction [1–16]. However, since plasma produces heat, radicals, excited species, ions/electrons, and other intermediate species simultaneously, one of the major challenges is to decouple the complex plasma-flame interaction so that the contribution of individual species produced by plasma to combustion enhancement can be understood

* Corresponding author.
E-mail address: yju@princeton.edu (Y. Ju).

1540-7489/$ - see front matter © 2010 The Combustion Institute. Published by Elsevier Inc. All rights reserved.
doi:10.1016/j.proci.2010.06.148

quantitatively at the elementary reaction level. As such, it is of great importance to develop a well-defined plasma-flame system that is simple to model and can provide quantitative experimental data to understand the effect of plasma generated species.

Much work has been conducted recently to understand the role of plasma generated species on ignition, flame stabilization, and extinction. For ignition studies, the reduction of ignition temperature was confirmed and analyzed in a counterflow burner with the activation by a magnetic gliding arc [1]. The catalytic effect of NO_x on ignition enhancement was quantitatively examined. The reduction of ignition delay time by a non-equilibrium plasma discharge was also measured in Refs. [11,17]. The results showed that the ignition delay times could be decreased by about an order of magnitude. An increase of atomic oxygen concentration was observed and was used as an explanation for the decrease of ignition delay times.

Unfortunately, for plasma assisted flame speed and extinction limit enhancement, few quantitative experiments have been conducted. Recently, quantitative understanding of the enhancement mechanism of flame speed by plasma produced species has been investigated by several research groups [12,15,16]. Ombrello and co-workers isolated singlet oxygen ($O_2(a^1\Delta_g)$) and ozone (O_3) effects and demonstrated that both (at concentrations of several thousand ppm) enhanced flame speeds by a few percent [15,16]. The experimental data further showed that the current kinetic model for $O_2(a^1\Delta_g)$ significantly over-predicted the enhancement for hydrocarbon flames. Enhancement of flame stability by non-equilibrium plasma discharge and an electric field also has been observed for lifted flames [13,14,18]. Differing explanations have been given based on the production of H_2 and CO as well as on H and O and on the ionic wind.

Contrary to the previous explanation of the mechanism of plasma assisted combustion, a recent study of extinction limit enhancement by a non-equilibrium gliding arc with Rayleigh scattering and laser induced fluorescence measurements of temperature and OH concentration, respectively, [2] showed that the extinction limit enhancement by a low temperature gliding arc discharge was only a thermal effect. However, a nano-second repetitive discharge produces atomic oxygen efficiently; this, coupled with an increase in temperature as well as the decrease of pressure may slowdown radical recombination to a sufficient degree which may allow the observation of kinetic enhancement to extinction limit. The question becomes whether the effect of atomic oxygen on flame extinction is different at higher atomic oxygen concentrations and elevated temperatures. If so, how do we quantitatively demonstrate and understand this effect in a well defined experiment?

The goal of the present study was to develop a sub-atmospheric pressure counterflow burner integrated with a nano-second non-equilibrium plasma system to decouple the plasma-flame interaction and reduce radical quenching. This system will provide a tool to answer the above questions and to study the effects of atomic oxygen production on the extinction limit.

2. Experimental method

2.1. Counterflow flame and nano-second pulsed discharge systems

A schematic of the experimental system is shown in Fig. 1. The experimental setup consisted of a counterflow burner, which was located in a low pressure chamber of 406 mm diameter and 629 mm height. The inner tubes of the counterflow burners were 20 mm inner diameter, and the outer tubes of the inert argon curtain were 28 mm inner diameter; both were made of quartz. The separation distance of the oxidizer and fuel burner nozzles was 20 mm. The argon flow isolated the flame from the environment and provided cooling for the burner. A honeycomb plate was placed inside the tube to ensure a uniform flow field at the nozzle exit. Two parallel bare copper electrodes were located inside the tubes of the upper (oxidizer side) burner and the ends of the electrodes were 10 mm away from the nozzle exit to avoid electric interaction with the thermocouple and allow the diffusion to smooth any non-uniformity till the nozzle exit. Because the pressure of the experiments is very low, diffusion is fast and the effect of the electrode inside the tube on the flow field near the centerline of the burners is negligible. The electrodes were 15×22 mm in dimension and the edges were smoothed to avoid the concentration of electric field and spark breakdown. The separation distance between the two

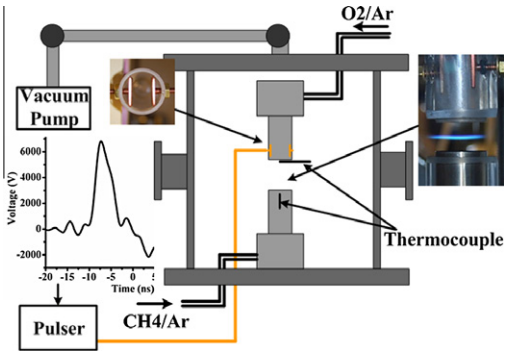

Fig. 1a. Schematic of experimental setup.

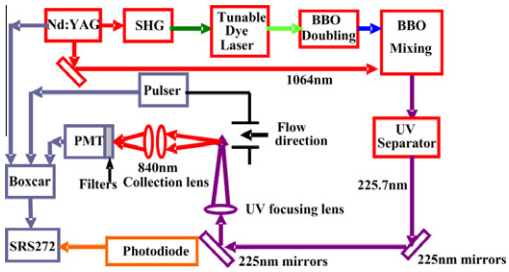

Fig. 1b. Schematic of the TALIF setup for atomic oxygen measurement.

electrodes was 10 mm. A nano-second pulse generator (FID FPG 30-50MC4) was used to generate the non-equilibrium plasma; this device is capable of producing 32 kV pulses with individual pulse duration of 6 ns (full width at half maximum, FWHM). To examine the effect of the plasma repetition rate, the frequency of the pulser was adjusted up to 40 kHz. A typical pulse voltage waveform, characterized with the aid of a LeCroy high voltage probe (PPE20KV), is embedded in Fig. 1a. The current through the electrodes was measured with a Pearson Coil (Model 6585). The energy supplied to the discharge per pulse was estimated by the integration of the voltage and current in terms of time. The energy provided to the discharge is approximate 0.67 mJ per pulse, corresponding to average power of 3.4, 13.4 and 26.8 W at 5, 20 and 40 kHz repetition frequency, respectively. During the experiments, the peak amplitude of the voltage was fixed at 7 kV as shown in Fig. 1a.

At first, a nano-second pulsed non-equilibrium plasma system was integrated with the counter-flow diffusion flame burner [1,2,19,20]. The O_2/Ar ratio was fixed at 0.28:0.72, while the CH_4 concentration in Ar varied from 0.3 to 0.36. The pressure was held constant at 8 kPa. The extinction strain rates were then measured by fixing the fuel mole fraction and gradually increasing the flow velocity until extinction was observed. During the experiments, momentum balance between the two nozzles was always maintained to keep the stagnation plane and the flame in the center of the two burner nozzles. At the same time, temperatures were measured by two thermocouples at the exits of the two burners with careful consideration of electric field interaction (In order to avoid the interaction of electric field to the thermocouples, the electrodes inside the tube were located 10 mm away from the nozzle exit where the thermocouple was located to measure the oxidizer boundary temperature. The thermocouple measurement was also confirmed by the NO thermometry method [21] and they were in good agreement. Because of the simplicity and frequent measurements of the temperature, thermocouple measurement was employed in this paper). Then, a Xe calibrated two photon absorption laser induced fluorescence (TALIF) method was used to measure the absolute atomic oxygen concentrations at the burner exit. After that, the flame extinction was modeled using the measured flow temperature with atomic oxygen concentration, and the kinetic pathways were analyzed.

2.2. Two-photon absorption laser induced fluorescence (TALIF) system

A plasma discharge in Ar/O_2 mixtures can generate electrons, ions, atomic oxygen, O_3, electronically and vibrationally excited O_2, and excited Ar. In our experiments, the focus is on the role of atomic oxygen, which is one of the most important radicals produced by nano-second plasma. A TALIF system, calibrated using a Xe reference measurement, was used to determine the absolute atomic oxygen concentration at the oxidizer-side burner exit [8]. The schematic of the TALIF system is shown in Fig. 1b. An Nd:YAG laser was used to generate 532 nm radiation to pump a tunable dye laser that was tuned to 573 nm. To produce the required 226-nm radiation, this 573 nm beam was frequency doubled and then frequency mixed with the 1064 nm output of the Nd:YAG laser. The TALIF fluorescence was observed using an 850 nm bandpass filter of 40 nm FWHM and a Hamamatsu photomultiplier (PMT-R7154). Atomic oxygen was measured at the oxidizer side exit of the burner. Using a 300 mm focal length lens, the 10-μJ/pulse UV beam was focused 30 mm ahead of the probe volume (the center of the burner) to avoid saturation. The signal was recorded at the center of the burner exit and ~3 mm from the burner exit, which is well away from the flame. The gap between the parallel electrode plates is 10 mm. The signal was averaged over this distance. The dye laser was scanned in wavelength to characterize the atomic oxygen fluorescence spectrum. A separate vacuum cell was used to obtain the two photon fluorescence spectrum of Xe. Corrections for the transmission of the vacuum cell and bandpass filter were made to find the atomic oxygen density by the method described in Refs. [8,22].

3. Results and discussion

3.1. Uniform nano-second non-equilibrium pulsed discharge

The pulser used in this study has a very short duration that results in a high *reduced electric field* (characterized by the E/N ratio, where E is the electrical field and N is the neutral gas density); high values of E/N can greatly improve the uniformity and stability of the plasma [5,23] and pro-

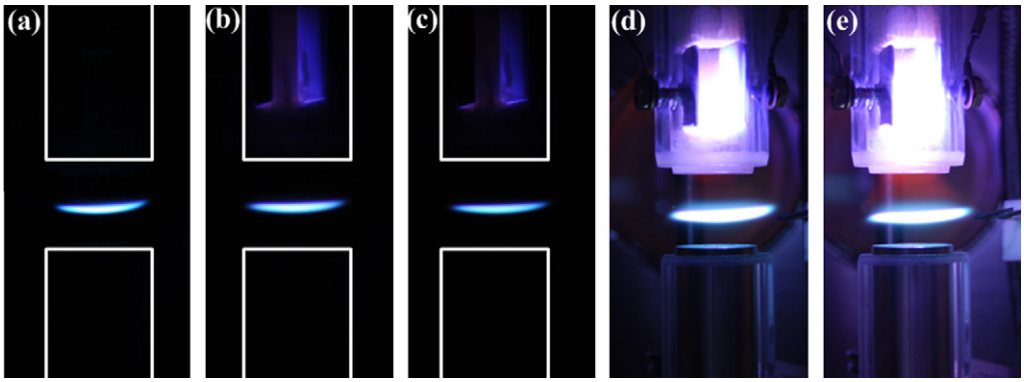

Fig. 2. Images of flames at $X_{CH4} = 0.36$, $X_{O2} = 0.28$ with balance of argon, a = 178 s^{-1}, d = 20 mm, P = 8 kPa (a) without discharge (b) $f = 5$ kHz (c) $f = 10$ kHz (d) $f = 20$ kHz (e) $f = 40$ kHz.

duce efficient ionization, electronic excitation, and dissociation of molecular species, such as oxygen, by direct electron impact [24]. Figure 2a–e shows images of flames with and without the nano-second non-equilibrium pulsed discharge at 8 kPa. The pulser repetition frequencies were increased from 5 to 40 kHz. The discharge was uniform in the transverse direction of the electrodes and no visible filamentary structure was observed for repetition frequency from 5 to 40 kHz. Figure 2d and e show a visible plasma jet issuing from the burner exit and reaching the reaction zone. The pulsed discharge in Ar/O_2 produces excited Ar (Ar^*), as well as multiple oxygen containing species including O, O_3, $O_2(v)$, $O(^1D)$, $O(^1S)$, $O_2(a^1\Delta_g)$, $O_2(b^1\Sigma_g)$, etc. It is clear that $O_2(a^1\Delta_g)$ and $O_2(b^1\Sigma_g)$ have longer lifetimes compared to other electronically excited species (see Ref. [15,16] for related quenching rates). These two species have low excitation energy (0.98 and 1.6 eV, respectively) and can emit photons at orange and red wavelengths (dimol emission of $O_2(a^1\Delta_g)$ [25]) when quenching occurs. It is also known that both excited and metastable Ar, which have an excitation energy of about 11 eV, and excited atomic oxygen emit radiation between 650 and 750 nm [26,27]. Overall, the emission in the afterglow of an Ar/O_2 discharge is produced from the relaxation processes of excited species like Ar^*, $O(^1D)$, $O(^1S)$, $O_2(a^1\Delta_g)$, and $O_2(b^1\Sigma_g)$. During the relaxation processes, ground state atomic oxygen can be produced. Therefore, the visible emission indicates that there exist significant concentrations of excited species, radicals, and atoms between the nozzle exit and the reaction zone that need to be quantitatively examined.

3.2. TALIF measurements of absolute concentration of atomic oxygen

Simplified energy level diagrams of O and Xe are given in Refs. [22,28]. The ground state of atomic oxygen can be excited by absorbing two photons at a wavelength of 225.7 nm. The transition between the excited 3p ^3P and the 3 s ^3S states will release a single photon at 844.6 nm. For Xe the two photon absorption from $5p^6$ $^1S_0$ to 6p′[3/2]2 states is at 224.31 nm, and the de-excitation to 6s′ [1/2]1 occurs at 834.91 nm. The advantage of the Xe calibration strategy is that both the absorbing and the fluorescence wavelengths of each species are close to each other, so that there is no need to modify either the focusing optics, collection bandpass filter, or the PMT.

In order to achieve a better signal of atomic oxygen, the PMT was placed inside the vacuum chamber. The UV beam was introduced into the chamber through a fused silica window. The number density of atomic oxygen N_O was calculated using the following equation in terms of the known number density of Xe, N_{Xe},[8]

$$N_O = \frac{S_O}{S_{Xe}} g_{ND} \frac{a_{21}(Xe)}{a_{21}(O)} \left(\frac{\sigma^{(2)}(Xe)}{\sigma^{(2)}(O)}\right) \left(\frac{\upsilon_O}{\upsilon_{Xe}}\right)^2 \times \frac{1}{F_O(T)} N_{Xe} \quad (1)$$

where S_o and S_{Xe} are the observed fluorescence signals for O and Xe, respectively, a_{21} the fluorescence quantum yields, $\sigma^{(2)}$ the two photon absorption cross sections, $F_O(T)$ the atomic oxygen Boltzmann factor of the probed state, and υ the photon energies [8].

The dependence of the measured atomic oxygen concentration on the pulse repetition frequency is plotted in Fig. 3 where it is shown that atomic oxygen concentration increased with the increase of the pulse repetition rate. For repetition rates below 5 kHz, atomic oxygen concentration was very low. A previous study by Uddi et al. [28] showed that the characteristic decay time of atomic oxygen in O_2/He plasma at 8 kPa and 300 K was ~3 ms. In this experiment, the distance between the end of electrodes in the burner

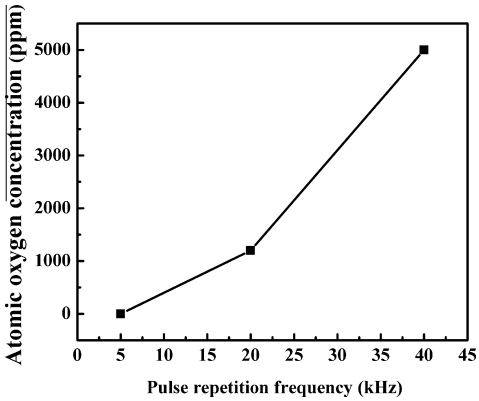

Fig. 3. Dependence of average atomic oxygen concentration at the burner exit on the pulse repetition frequency.

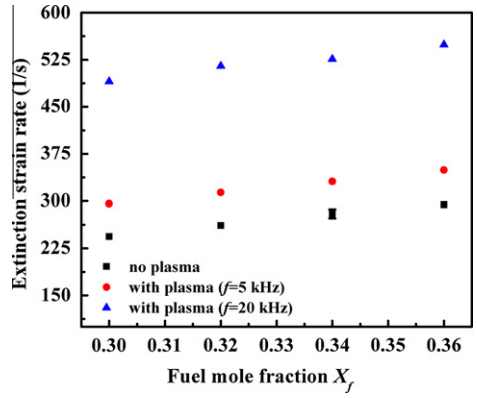

Fig. 4. Dependence of extinction strain rate on fuel mole fraction for different plasma repetition rates at 8 kPa.

to the exit of the burner is 1 cm, and the characteristic flow velocity in our experiments is ~100 cm/s. Therefore, the residence time is approximately 10 ms. As such it is probable that the atomic oxygen generated by the discharge already decayed to a concentration not detectable by TALIF before reaching the exit of the burner. However, when the repetition frequency was increased to 40 kHz, $N_O \approx 1.1 \times 10^{16}$ cm^{-3} (5000 ppm) at the burner exit. The increase in atomic oxygen concentration originates mainly from the increase of electron number density and also from the increase of the discharge temperature as well as the decrease of flow residence time. Note that at a higher repetition frequency, a higher flow velocity is required to reach flame extinction. In order to adapt the flow conditions for extinction measurements, the flow velocity for 5 and 20 kHz was 100 cm/s, while for 40 kHz it was 200 cm/s.

3.3. Enhancement of flame extinction limit

The extinction strain rates of CH_4/O_2 diffusion flames were measured with and without plasma ($f = 5$ and 20 kHz). A definition of global strain rate [29]

$$a_O = \frac{2U_O}{L}\left(1 + \frac{U_f\sqrt{\rho_f}}{U_O\sqrt{\rho_O}}\right) \quad (2)$$

was adopted and compared with numerical simulations. Here U is the flow velocity, ρ the flow density, and L the separation distance between the two burner nozzles. The subscripts o and f refer to the oxidizer and fuel sides, respectively. Figure 4 shows the dependence of extinction strain rates on fuel mole fraction with and without plasma discharge at different repetition plasma rates at 8 kPa. It is shown that the extinction strain rate increased with the increase of fuel mole fraction. In addition, with the increase of the pulse repetition frequency, Fig. 4 shows a significant increase of extinction limit enhancement. The enhancement of the extinction limit for $f = 5$ kHz is about 25%, while for $f = 20$ kHz the enhancement was approximately 90%.

In order to understand the mechanism of the extinction limit enhancement, we did the following: (1) measure the extinction limit by raising the oxidizer temperature via an electrical heater without plasma; and (2) compute the extinction limit with the measured temperature and atomic oxygen concentration at the oxidizer nozzle exit. By comparing these additional experimental and numerical results with the baseline extinction limit, we can understand to what extent the observed extinction limit enhancement was from the thermal and the kinetic mechanisms. The measured oxidizer temperatures at the repetition frequency of $f = 5$ and 20 kHz were 398 and 528 K, respectively.

Figure 5 shows the comparison of the measured extinction limits with the nano-second

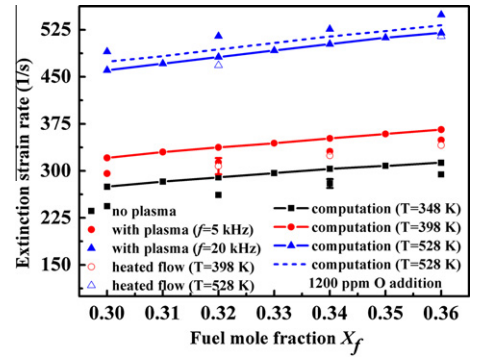

Fig. 5. Comparisons of extinction strain rates between experimental results with plasma activation and an electrically heated flow as well as numerical simulations at 8 kPa.

plasma discharge and the electrical heater set to the same temperatures as well as the simulation results with (dashed line) and without (solid line with symbols) atomic oxygen production for repetition rates of $f = 20$ kHz at 8 kPa. The measurements showed that for the repetition rate of 5 kHz, the enhancement by the nano-second discharge and the electrical heater at the same oxidizer temperature of 398 K were approximately equal. This result implies that the enhancement at a low pulse frequency was predominately a thermal effect. This result is reasonable because the TALIF measurements (see Fig. 3) showed that there was little atomic oxygen at the exit of the burner when the repetition frequency was 5 kHz. However, when the repetition rate was increased to 20 kHz, Fig. 5 shows that the extinction limit by nanosecond plasma was about 10% higher than that by the electrical heater at the same oxidizer temperature of 528 K, indicating that the existence of atomic oxygen may enhance the extinction limit by promoting the chain-branching reactions. The extinction limit of plasma assisted CH_4-air combustion was modeled using the measured atomic oxygen concentration and the temperature using OPPIDIFF of the CHEMKIN package [30] with a modified arc-length continuation method [20] for plug flow with USC Mech II [31]. All the simulations were performed at 8 kPa with a fixed fuel stream temperature at 300 K. The temperatures of the oxidizer side was set as 528, 398, and 348 K, respectively, for plasma discharge frequencies of $f = 20$ and 5 kHz and without the activation by plasma. The atomic oxygen concentration with plasma discharge at 20 kHz was 1200 ppm (the uncertainty of the TALIF measurement is approximately 40% [8], 40% increase of atomic oxygen concentration in calculation resulted an increase of extinction strain rate by less than 0.5%). The results are also plotted in Fig. 5. The figure shows that the model well reproduced the extinction limit without plasma discharge. The results also show that at 20 kHz, the predicted kinetic enhancement by 1200 ppm atomic oxygen addition was only 2.5%, which was much below the kinetic enhancement observed in the experiment, suggesting the presence of additional kinetic enhancement pathways. The above comparison demonstrates clearly that non-equilibrium plasma discharge can enhance flame stabilization kinetically via the production of atomic oxygen and other excited species.

To further understand the effects of atomic oxygen addition and oxidizer temperature on the extinction limits, extinction strain rates were computed at different oxidizer temperatures (but constant fuel side temperature of 300 K) and atomic oxygen concentrations at constant pressure of 8 kPa. As shown in Fig. 6, the extinction strain rates increases substantially with the increase of oxidizer temperature and atomic oxygen concentration. The results also reveal that at higher oxidizer temperature, the kinetic enhancement of atomic oxygen becomes more significant. Figure 7 shows the detailed atomic oxygen profiles at the extinction limits for different oxidizer temperatures with 5000 ppm atomic oxygen addition at the oxidizer side at 8 kPa. Here, the fuel-side origin is located at $x = 0$ cm, and the oxidizer-side origin is located at $x = 2$ cm. The figure shows that with the increase of oxidizer temperature, more atomic oxygen could be transported to the reaction zone. At 900 K, nearly 80% of atomic oxygen could reach the reaction zone to enhance the flame. With a further increase of temperature to 1000 K, a significant increase of radical production is predicted. Therefore, there is a crossover temperature between 900 and 1000 K that governs the transition from radical termination to branching process.

To understand the transition process from radical termination to branching with atomic oxygen

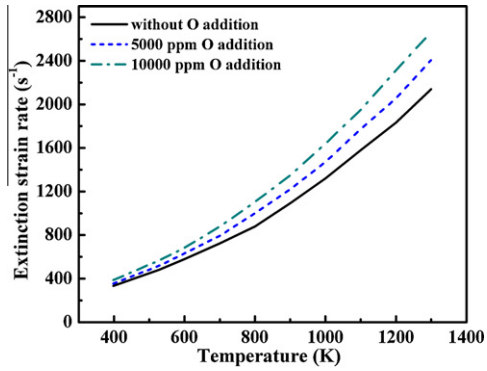

Fig. 6. Simulation of the dependence of extinction strain rates on oxidizer-side temperatures with and without atomic oxygen addition.

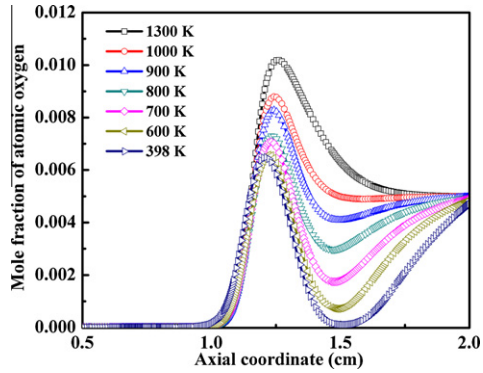

Fig. 7. Distributions of atomic oxygen mole fraction in the flame zone and on the side of oxidizer stream for different temperatures with 5000 ppm atomic oxygen addition at the extinction limits.

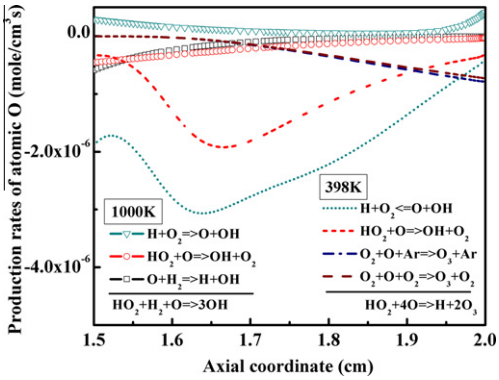

Fig. 8. Calculated rates of elementary reactions related to atomic oxygen consumption and production with oxidizer temperatures at 398 K (dashed line) and 1000 K (solid line), respectively, and 5000 ppm atomic oxygen addition (oxidizer exit at 2 cm) at 8 kPa.

addition, the consumption and production pathways of the atomic oxygen and related radicals were analyzed at the preheat zone for two different temperatures, 398 and 1000 K, with 5000 ppm atomic oxygen addition. The major consumption and production paths of atomic oxygen at these two temperatures are shown in Fig. 8 (solid line with symbols for 1000 K and dashed line for 398 K). The above pathways represent 90% of the atomic oxygen consumption. At 398 K, the major atomic oxygen consumption reactions were $O + OH = H + O_2$, $HO_2 + O = OH + O_2$ and the two recombination reactions from O and O_2 to O_3. The summation of these four reactions leads to a global reaction of $HO_2 + 4O = H + 2O_3$. This result indicates clearly that at low temperatures atomic oxygen is terminated to form O_3. However, Fig. 8 shows that at 1000 K the addition of atomic oxygen promotes the chain branching reactions $O + H_2 = H + OH$ and $O + H_2 = H + OH$ as well as the chain propagation reactions and $HO_2 + O = OH + O_2$. The overall reaction becomes $HO_2 + H_2 + O = 3OH$, which implies that the addition of one O atom converts the less reactive radical HO_2 and H_2 (which originates from the fuel leakage near the extinction limit) to three active OH radicals. Therefore, the kinetic enhancement of atomic oxygen production from plasma has different impacts on extinction limit enhancement, depending strongly on the temperature. Figures. 7 and 8 show that there is a crossover temperature between 900 and 1000 K, above (below) which the kinetic enhancement by atomic oxygen production is governed by chain-branching (chain termination) reactions. The above analysis and experimental results provide a good explanation to the controversial conclusions made for different experimental conditions for plasma assisted flame speed enhancement.

4. Conclusion

A well-defined platform to study the effect of atomic oxygen production by non-equilibrium plasma on the extinction limits was developed by integrating a counterflow burner with a nano-second pulsed discharge. Low pressure experiments demonstrated that the increase of plasma repetition rate increased dramatically the extinction limit of Ar diluted CH_4/O_2 diffusion flames. The TALIF measurement of absolute concentration of atomic oxygen showed that the atomic oxygen production also increased with the increase of plasma repetition rate, and at a pulse repetition rate of 20 kHz, the concentration of atomic oxygen was observed to be 1200 ppm; this value was also employed in numerical simulations as a boundary condition. Comparison between plasma assisted combustion and electrically heated combustion at the same temperature confirmed that at low pulse repetition rate the enhancement of extinction limit was dominantly thermal, but that there was a kinetic effect of the atomic oxygen at a high pulse repetition rate. Moreover, the comparison between experiment and numerical modeling with the measured temperature and atomic oxygen concentration suggests that there were possibly additional kinetic effects from other excited species. Numerical simulations and kinetic path analysis further revealed that at higher temperature, more atomic oxygen can be transported to the reaction zone to enhance the flame. There is a crossover temperature between 900 and 1000 K, above (below) which the kinetic enhancement by atomic oxygen production is governed by chain-branching (chain termination) reactions. The present results provide a good explanation to the conclusions made in different experimental conditions for plasma assisted flame speed enhancement and suggest that in order to achieve a significant kinetic enhancement of flame stabilization from atomic oxygen, the plasma discharge or gas flow temperature needs to be above the critical crossover temperature.

Acknowledgments

This work was supported by the MURI research grant from the Air Force Office of Scientific Research and the grant FA9550-07-1-0136 under the technical monitor of program manager Dr. Julian Tishkoff. Part of the research was performed while one of the authors (Timothy Ombrello) held a National Research Council Research Associateship Award at the United States Air Force Research Laboratory, Wright-Patterson Air Force Base. The authors also with to thank Mr. Tim Bennett from the Department of Mechanical and Aerospace Engineering, Princeton University for the technical support.

References

[1] T. Ombrello, Y. Ju, A. Fridman, *AIAA Journal* 46 (10) (2008) 2424–2433.
[2] T. Ombrello, X. Qin, Y. Ju, A. Gutsol, A. Fridman, C. Campbell, *AIAA Journal* 44 (1) (2006) 142–150.
[3] S.A. Bozhenkov, S.M. Starikovskaia, A.Y. Starikovskii, *Combust. Flame* 133 (2003) 133–146.
[4] A.Y. Starikovskii, N.B. Anikin, I.N. Kosarev, E.I. Mintoussov, S.M. Starikovskaia, V.P. Zhukov, *Pure Appl. Chem.* 78 (6) (2006) 1256–1298.
[5] S.M. Starikovskaia, *J. Phys. D Appl. Phys.* 39 (2006) R265–R299.
[6] G. Lou, A. Bao, M. Nishihara, et al., *Proc. Combust. Inst.* 31 (2007) 3327–3334.
[7] E. Mintusov, A. Serdyuchenko, I. Choi, W.R. Lempert, I.V. Adamovich, *Proc. Combust. Inst.* 32 (2009) 3181–3188.
[8] M. Uddi, N. Jiang, E. Mintusov, I.V. Adamovich, W.R. Lempert, *Proc. Combust. Inst.* 32 (2009) 929–936.
[9] S.V. Pancheshnyi, D.A. Lacoste, A. Bourdon, C.O. Laux, *IEEE Trans. Plasma Sci.* 34 (6) (2006) 2478–2487.
[10] N. Chintala, R. Meyer, A. Hicks, et al., *J. Propul. Power* 21 (2) (2005) 583–590.
[11] I.N. Kosarev, N.L. Aleksandrov, S.V. Kindysheva, S.M. Starikovskaia, A.Y. Starikovskii, *J. Phys. D Appl. Phys.* 41 (2008), 032002(1–6).
[12] A.M. Starik, V.E. Kozlov, N.S. Titova, *Combust. Flame* 157 (2) (2009) 313–327.
[13] W. Kim, M.G. Mungal, M.A. Cappelli, *Combust. Flame* 157 (2) (2009) 374–383.
[14] G. Pilla, D. Galley, D.A. Lacoste, F. Lacas, D. Veynante, C.O. Laux, *IEEE Trans. Plasma Sci.* 34 (6) (2006) 2471–2477.
[15] T. Ombrello, S.H. Won, Y. Ju, S. Williams, *Combust. Flame* 157 (10) (2010) 1906–1915.
[16] T. Ombrello, S.H. Won, Y. JU, S. Williams, *Combust. Flame* 157 (10) (2010) 1916–1928.
[17] N.L. Aleksandrov, S.V. Kindysheva, I.N. Kosarev, S.M. Starikovskaia, A.Y. Starikovskii, *Proc. Combust. Inst.* 32 (2009) 205–212.
[18] S.H. Won, M.S. Cha, C.S. Park, S.H. Chung, *Proc. Combust. Inst.* 31 (2007) 963–970.
[19] A. Fridman, A. Gutsol, S. Gangoli, Y. Ju, T. Ombrello, *J. Propul. Power* 24 (6) (2008) 1216–1228.
[20] Y. Ju, H. Guo, K. Maruta, *J. Fluid Mech.* 23 (1997) 315–334.
[21] W.G. Bessler, C. Schulz, V. Sick, J.W. Daily, in: *Proceedings of the Third Joint Meeting of the U.S. Sections of The Combustion Institute*, March 2003, Chicago, USA, Paper PI05.
[22] K. Niemi, V. Schulz-von der Gathen, H.F. Dobele, *Plasma Sources Sci. T* 14 (2005) 375–386.
[23] A.Y. Starikovskii, *Proc. Combust. Inst.* 30 (2005) 2405–2417.
[24] A. Bao, Y. G Utkin, S. Keshav, G. Lou, I.V. Adamovich, *IEEE Trans. Plasma Sci.* 35 (6) (2007) 1628–1638.
[25] M.V. Zagidullin, V.D. Nikolaev, M.I. Svistun, N.A. Khvatov, E.V. Fomin, *Opt. Spectrosc.* 105 (2) (2008) 202–207.
[26] S. Wang, V. Schulz-von der Gathen, H.F. Döbele, *Appl. Phys. Lett.* 83 (16) (2003) 3272–3274.
[27] W.T. Sun, G. Li, H.P. Li, et al., *J. Appl. Phys.* 101 (2007), 123302(1-6).
[28] M. Uddi, *Non-equilibrium kinetic studies of repetitively pulsed nanosecond discharge plasma assisted combustion*, PhD thesis, Ohio State University, Columbus, OH, 2008.
[29] K. Seshadri, F.A. Williams, *Int. J. Heat Mass Transfer* 21 (1978) 251–253.
[30] R.J. Kee, F.M. Rupley, J.A. Miller, et al., *Chemkin Collection, Release 3.7.1*, Reaction Design, Inc., 2003, San Diego, CA.
[31] H. Wang, X. You, A.V. Joshi, et al., available at <http://ignis.usc.edu/USC_Mech_II.htm>.